2012-12-11

Characterization of Ru Thin-Film Conductivity upon Atomic Layer Deposition on H-Passivated Si(111)

K. Roodenko, *et al*

AIP | Journal of Applied Physics

Characterization of Ru thin-film conductivity upon atomic layer deposition on H-passivated Si(111)

K. Roodenko, S. K. Park, J. Kwon, L. Wielunski, and Y. J. Chabal

Citation: J. Appl. Phys. **112**, 113517 (2012); doi: 10.1063/1.4766747
View online: http://dx.doi.org/10.1063/1.4766747
View Table of Contents: http://jap.aip.org/resource/1/JAPIAU/v112/i11
Published by the AIP Publishing LLC.

Characterization of Ru thin-film conductivity upon atomic layer deposition on H-passivated Si(111)

K. Roodenko,[1] S. K. Park,[1] J. Kwon,[1] L. Wielunski,[2] and Y. J. Chabal[1]
[1]*Materials Science and Engineering Department, University of Texas at Dallas, Richardson, Texas 75080, USA*
[2]*Department of Physics and Astronomy, Rutgers University, Piscataway, New Jersey 08854, USA*

(Received 17 August 2012; accepted 9 October 2012; published online 11 December 2012)

The sheet resistance measured by a four-probe technique is compared to the resistivity data derived from the optical response of thin ruthenium films grown on hydrogen-passivated Si(111) surfaces by atomic-layer deposition using cyclopentadienyl ethylruthenium dicarbonyl, $Ru(Cp)(CO)_2Et$ and O_2 as gas reactant. The Drude-Landauer theory is applied to evaluate the spectroscopic ellipsometry response and the DC resistivity evaluated by 4-point probe measurements. Results indicate that thin Ru films (below ~5 nm) deposited on Si exhibit a higher sheet resistance than similarly grown Ru films on TiN. This is explained by an island-growth mechanism at the initial stages of Ru deposition that greatly diminishes the film conductivity before the formation of a continuous film. © *2012 American Institute of Physics*. [http://dx.doi.org/10.1063/1.4766747]

I. INTRODUCTION

Atomic layer deposition (ALD) is a growth technique that allows highly conformal deposition of thin films with atomic-level thickness control. ALD deposition of Ru had been recently explored using a variety of precursors and reactants.[1–3] The interest in Ru deposition arises from its high work function, low bulk resistivity, and ability to form stable conductive oxides. In this manuscript, we investigate the electrical characteristics (conductivity) of ultra-thin Ru films on H-passivated Si surfaces as a function of the number of Ru ALD cycles. We correlate results based on the optical Drude response, derived by fitting ellipsometric data, with direct sheet-resistance measurements obtained by electric four-point probe (FPP) measurements.[4]

Ellipsometry allows an indirect evaluation of the DC-resistivity. The optically determined DC-resistivity (ρ_{opt}) can be calculated based on the fitted components of the dielectric function. The dielectric function can be modeled using the form of Lorentzian oscillator model with the Drude term for conductivity Eq. (1)

$$\varepsilon(w) = \varepsilon_\infty - \frac{w_p^2}{w^2 - i\Gamma_D w} + \sum_k f_k \frac{w_{0k}^2}{w_{0k}^2 - w^2 + i\Gamma_k w}, \quad (1)$$

where ε_∞ is a high-frequency dielectric function, w_p the plasma frequency, Γ_D the Drude-term damping factor, f_k the Lorentz-term oscillator strength, w_{0k} the resonance frequency of the kth oscillator, and Γ_k the related damping factor.[5,6] The complex refractive index $n^*(w)$ is related to the complex dielectric function $\varepsilon = \varepsilon_1 + i\varepsilon_2$ through $(n^*(w))^2 = \varepsilon(w)$.

The knowledge of the Drude parameters w_p and Γ_d allows to estimate the DC-resistivity of the measured layer.[7] In an ideal metal with all electrons free, the unscreened plasma frequency is given by[8,9]

$$w_p^2 = \frac{4\ \pi\ N\ e^2}{m^*}, \quad (2)$$

where N is the density of the valence electrons, m* is the effective electron mass, and e is the effective electron charge. The optical conductivity is given by[8,9]

$$\sigma_{opt} = \frac{N\ e^2\tau}{m^*}, \quad (3)$$

where the scattering time τ is related to the Drude oscillator parameter Γ_d (in eV units) through $\Gamma_d = \frac{1}{\tau}$. The resistivity is inversely proportional to σ_{opt}, and given by $\rho_{opt} = \frac{1}{\sigma_{opt}}$.

The problem becomes more complex when the metal layer is not continuous, as in the case of materials that exhibit island-growth regime. In this case, fitting of the dielectric function requires an effective-medium approach that takes into account metallic islands and the material between these islands, for example, air. Evaluation of the resistivity thus should take into account the overall composition of this layer. Landauer *et al.*[10] have treated the problem of the conductivity of binary metallic mixtures, whose solution is given in Eq. (4)

$$\sigma_m = \frac{1}{4}\left[(3f_2 - 1)\sigma_2 + (3f_1 - 1)\sigma_1 + \sqrt{\left((3f_2 - 1)\sigma_2 + (3f_1 - 1)\sigma_1\right)^2 + 8\sigma_1\sigma_2}\right], \quad (4)$$

where f_1 and f_2 are the fractions of the inclusions of conductivities σ_1 and σ_2, respectively. Landauer *et al.*[10] had applied the theory to several binary metallic mixtures and found out that the theory explains well the variation of the resistivity as a function of composition for a variety of materials. In this article, we compare the values for the sheet resistance as derived from the direct electric four-point probe measurements with the ρ_{opt} values derived from the ellipsometric data and evaluated using Landauer theory. Generally, our data indicate that for Ru thicknesses (as evaluated by Rutherford backscattering spectroscopy (RBS) with values below ~5 nm) the Ru layers exhibit higher sheet resistance than

values reported earlier for Ru grown on TiN[2]. Based on the earlier published IR and AFM data,[1] and the ellipsometric measurements reported in this article, we suggest that the island growth mechanism during the initial steps of ALD leads to a delay in the development of a continuous conductive Ru layer. This observation is consistent with the previous studies,[11] which indicate that the nucleation of Ru on the nitride (SiN_x) is faster in comparison to nucleation of Ru on SiO_2 surfaces.

Since the optical evaluation of the DC-resistivity ρ_{opt} is indirect, a thorough analysis of the ellipsometric data is required. Therefore, this manuscript is structured as follows: after the presentation of the experimental details in Sec. II, Sec. III describes in detail the evaluation of the ellipsometric data. To address the problems of extraction of the Drude parameters w_p, and Γ_D from the ellipsometric measurements as well as the thickness and composition of Ru/Si interfaces and of the rough Ru surfaces, Sec. III is divided into three subsections. Section III A discusses the evaluation of the Ru dielectric function in two regimes, the "ultrathin-film" regime (12–27 ALD cycles) and the "thick-film" regime (56–60 ALD cycles). Section III B presents a discussion of surface and interface composition, where the ellipsometric results are cross-referenced and supported by other surface-sensitive techniques, namely, the XPS and XRD. Finally, Sec. III C examines the resistivity of Ru films in both ultrathin and thick-film regimes, with a cross-reference to the 4-probe measurements of the Ru sheet resistance to the optically evaluated resistivity values (ρ_{opt}).

II. EXPERIMENTAL

Double-side polished Piranha-cleaned and subsequently hydrogen-terminated Si (111) surfaces (30 s etching in aqueous HF (20%) solution) were loaded into a home-made ALD reactor.[1] Ruthenium deposition was performed using a cyclopentadienyl ethylruthenium dicarbonyl [$Ru(Cp)(CO)_2Et$] precursor and O_2 gas as reactants. Purified nitrogen gas (O_2 concentration $< 1 \times 10^{-5}$ ppm) was used as carrier and purge gas during the process, except for the O_2 pulse. A full cycle was completed when an O_2 exposure was performed after the Ru exposure. RBS was performed *ex situ* with 2 MeV He ions at the Rutgers Laboratory for surface modification. For the RBS measurements, the detector was positioned at a 160° backscattering angle with respect to the surface normal to measure the Ru atom density. A Rigaku Ultima III XRD system was used for grazing incidence XRD for crystallinity study, while the surface and interface composition of the samples were studied by ex situ XPS using an Al Kα source (Perkin-Elmer 5300). All of the Ru3d data were fitted using doublets[12] with $Ru3d_{5/2}$ positioned at 280 eV and spin-orbit splitting of 4.22 eV with ratio of 2:3. Doniach-Sunjic function with the asymmetric parameter of 0.01 convoluted with Gauss broadening to account for XPS system resolution[13,14] was used to fit the Ru3d peaks.

The sheet resistance of the Ru films was measured at room temperature by the Alessi manual 4 point probe that uses a C4S probe head with 1 mm spacing between the Tungsten carbide probe tips. The metering was provided by a Keithly 2400 4-wire digital meter. The sheet resistance, obtained from the FPP measurements was calculated from[4]

$$\rho = 4.532\ R\ d_{Ru}, \tag{5}$$

where R is the resistance between the contacts as described in Ref. 4 and d_{Ru} is the Ru thickness calculated by taking into account both the ellipsometric value calculated using Eq. (1) and the data obtained from the RBS measurements, and averaging these two values. The error bars $\Delta\rho$ were calculated based on the three measurements of the resistance R at different spots across the sample, and taking into account the error bars of d_{Ru} obtained from RBS and ellipsometry.

A Jobin-Yvon Horiba Uvisel spectroscopic ellipsometer was used for *ex-situ* characterization of the samples in 0.6–6.5 eV spectral range (visible spectral range, thereafter referred to as VIS-ellipsometry). To model the data, an effective medium approach (EMA) based on the Bruggeman formulation[15,16] was assumed to simulate the multiphase layers. The upper layer (and a symmetric bottom layer) was considered to be composed of Ru with either air inclusions or organic inclusions (due to the remaining precursor[1]); the interface consisted of SiO_2 (dielectric function from Ref. 17 with Ru inclusions, and finally, 0.5 mm thick bulk Si (dielectric function from Refs. 17 and 18 was positioned in the center of this stack (see the left-side inset in Fig. 1). This model is justified by our earlier FTIR studies of Ru deposition on H-passivated Si, where the formation of SiO_2 was observed at the interface during Ru growth cycles.[1]

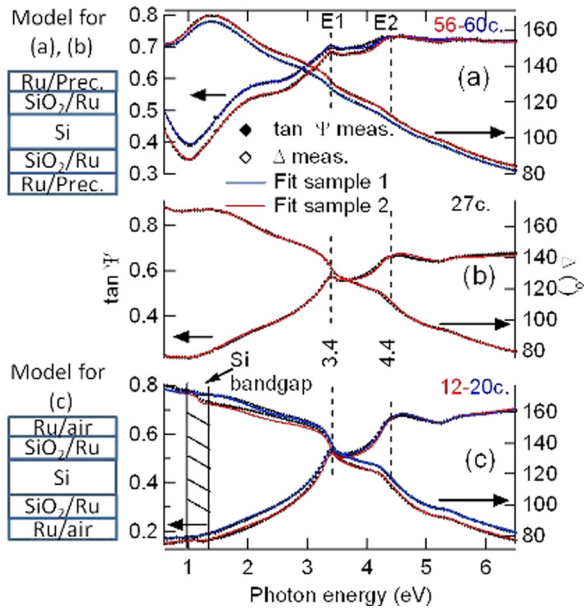

FIG. 1. Ellipsometric parameters tan ψ (left) and Δ (right) for (a) thick Ru films deposited using 56–60 ALD cycles; (b) 27-cycles ALD Ru film; and (c) Ru thin films by completion of 12 and 20 cycles, respectively. The measured data are shown by black dots. Plots (a) and (c) show *two* sets of data in the similar thickness range. Red: fit obtained from the sample in the *lower* number of ALD cycles. Blue: fit obtained from the sample in the *higher* number of ALD cycles. The left-side insets show schematic drawings of the layer-model that were used to fit the measured data. Upper inset: layer-model used for (a) and (b) with the precursor inclusions in the top Ru layer; Lower inset: layer-model used for (c) with the air inclusions in the top Ru layer.

To assess the level of reproducibility, each experiment was repeated several times and data analysis performed accordingly. In this manuscript, *two* spectra for *each* target Ru film thickness range (above 55 cycles and below 20 cycles) are presented for clarity. Both data sets were fitted *simultaneously* to obtain a consistent picture of the effective dielectric function. Only the thickness and EMA compositions were allowed to vary *separately* to fit the data, but the oscillator parameters were fitted to the *identical* values for both data sets. An intermediate thickness stage, obtained with 27-ALD cycles, is presented as well. The effective dielectric functions were modeled using the form of Lorentzian oscillators with the Drude term for conductivity Eq. (1).

Since effective medium approach gives a percentage $f_{Ru\ Interface}$ of Ru in Ru/SiO_2 interface and the percentage $f_{Ru\ top}$ of Ru in the top layer (see the model inset in Fig. 1), the ellipsometric thickness of Ru was calculated from

$$d_{Ru} = d_{Ru\ Interface}\, f_{Ru\ Interface} + d_{Ru\ top} f_{Ru\ top}, \qquad (6)$$

where $d_{Ru\ Interface}$ and $d_{Ru\ top}$ are the respective thicknesses of the interfacial and the top layers simulated by the effective medium approaches.

III. RESULTS AND DISCUSSION

The ellipsometric data obtained for all ALD-deposited films are shown in Fig. 1. All data exhibit features related to Si interband transitions, with the so-called critical points marked as E1 and E2 in Fig. 1.[19,20] The appearance of these critical points suggests that the signal from the substrate is not completely blocked by the ALD-deposited Ru films. The data obtained from the thinnest film (12 cycles, shown in red in Fig. 1(c)) include a feature associated with a 1.1 eV Si bandgap.[21] The appearance of this otherwise weak Si-bandgap related spectral feature is enhanced due to the fact that both Si surfaces are polished, allowing the light to be multiply-reflected at the interfaces. The 1.1 eV feature is well-reproduced by the model with a double-side polished Si substrate with symmetrically deposited Ru on both sides of the substrate as realized experimentally. This feature is not observable any longer for Ru films obtained after 20-cycles or more, due to the surface and interface roughening. As the amount of Ru increases, there is an apparent low-frequency Drude-like charge carrier response that develops at photon energies below 1.5 eV.

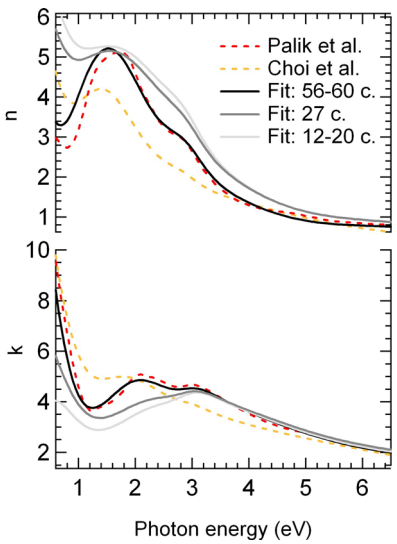

FIG. 2. Dielectric constants n, k of Ru as determined from literature[6,17] (shown in dashed red and orange) and the dielectric functions, n and k, derived for thin Ru films. The data is calculated based on the parameters given in Table 1. The Kramers-Kronig consistency is best observed expanding the photon-energy scale below 0.6 eV (not shown).

A. Dielectric functions

In this section, we give a detailed discussion concerning the fits of the components of the dielectric function parameterized in accordance with Eq. (1). This allows us to extract the Drude parameters, w_p and Γ_D from the ellipsometric measurements of Ru samples for further evaluation of the resistivity using the Landauer equation (ultimately presented in Sec. III C).

At the first attempt, two Ru dielectric functions were considered in our fits: the dielectric functions suggested by the Palik's Handbook of Optical Constants of Solids[17] and alternatively by Choi *et al.*[6] The dispersion of these dielectric constants n and k is reproduced in Fig. 2 in dashed red (data by Palik[17]) and orange (data by Choi *et al.*[6]) lines. One can observe considerable differences, especially in the lower spectral range (below 4 eV).

Using the layer-models shown in Fig. 1, the spectra of the Ru thin films were first fitted using either dielectric functions published by Choi *et al.*[6] or by Palik.[17] Both of these approaches worked well in the high energy range but failed to fit the data in the lower spectral range, at energies bellow ~2.5 eV. Keeping in mind the aforementioned wide variations

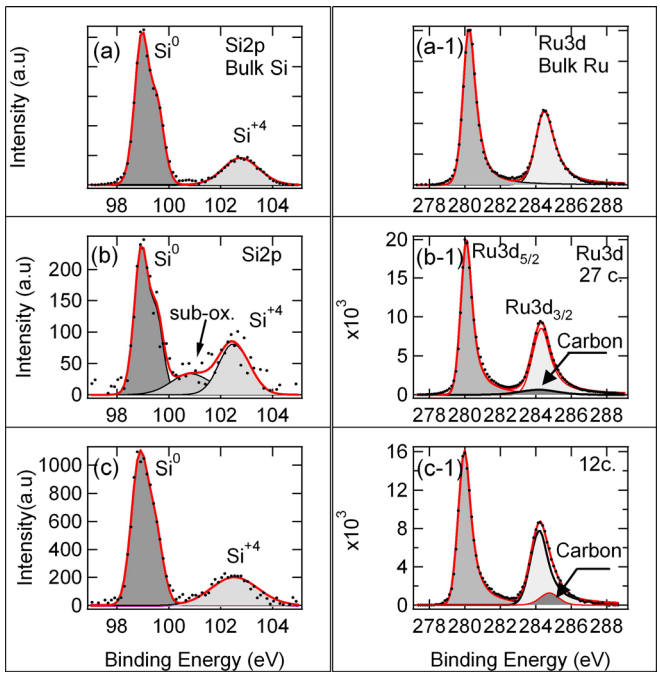

FIG. 3. XPS Si2p and Ru3d core-level data obtained from (a) and (a-1) bulk samples: unmodified piranha-cleaned SiO_2/Si sample and from sputter-cleaned bulk Ru sample, respectively; (b) and (b-1): 27 cycles Ru samples; (c) and (c-1): 12 cycles Ru samples. The superscript in Si^0 and Si^{+4} indicates the oxidation state of the deconvoluted Si components.

TABLE I. Oscillator parameters that were used to fit on the ellipsometric data shown on Fig. 1. The resulting n and k parameters are shown in Fig. 2. Published data by Choi *et al*. and the parameterized data from the "*Handbook of Optical Constants of Solids*" by Palik[17] are given for comparison. Choi *et al*.[6] do not list the parameters $\hbar\Gamma_d$, $\hbar w_p$. The tabulated data for these parameters were extracted from Fig. 3(a) in Ref. 6.

		Choi *et al*.[6]	Palik[17] (Parameterized)	Ru 56–60 c.	Ru 12–27 c.
	$\hbar\Gamma_d$ (eV)	7	6.75	7	4.20
Drude parameters	$\hbar w_p$ (eV)	0.3	0.14	0.15	0.25
	$\hbar w_1$ (eV)	0.6	0.5	0.58	0.62
	F_1	47.3	44	60	60
Oscillator #1	$\hbar\Gamma_1$ (eV)	1.1	0.9	1.2	0.8
	$\hbar w_1$ (eV)	1.8	2	1.95	2.1
	F_1	27.1	30	35	27
Oscillator #2	$\hbar\Gamma_1$ (eV)	1.7	1.5	1.5	1.8
	$\hbar w_1$ (eV)	2.9	3.0	2.9	2.9
	F_1	0.6	3.0	2.2	2.2
Oscillator #3	$\hbar\Gamma_1$ (eV)	0.8	0.9	0.7	0.7
	$\hbar w_1$ (eV)	4.1	4.3	4.15	4.15
	F_1	5	1.75	2.3	2.3
Oscillator #4	$\hbar\Gamma_1$ (eV)	4.5	2.9	2.3	2.3
	$\hbar w_1$ (eV)	…	7.1	6.95	6.8
	F_1	…	1.1	1.4	1.8
Oscillator #5	$\hbar\Gamma_1$ (eV)	…	5.0	5.5	5.5

in the published Ru dielectric functions, we parameterized the dielectric function found in Palik's Handbook of dielectric constants[17] using a Lorentz oscillator model, as suggested by Choi *et al*.[6] Next, allowing minimal variations in the oscillator parameters, the Drude parameters and film thicknesses were fitted using data obtained from the thick films (56–60 cycles). The result of the fit for the ellipsometric parameters tan Ψ and Δ is shown in Fig. 1(a) by blue and red lines, while the dielectric function obtained for Ru thin films is shown by a black continuous curve in Fig. 2. The resulting oscillator parameters are summarized in Table I, and Table II lists the parameters obtained for the thickness and EMA composition. To ensure consistency, the data sets obtained from *both* 56-cycle and 60-cycle samples were fitted *simultaneously* until convergence of the oscillator parameters and the Ru thicknesses was obtained. Fig. 2 shows that there is a good match in the higher energy spectral range (3.5–6.5 eV) with the literature values given by Choi *et al*.[6] or by Palik.[17] The major difference between our fits and the literature values is primarily in the 0.5–3.5 eV spectral range.

Next, thinner Ru films (12–27 cycles) were initially fitted using the effective dielectric function obtained from the fits of the 60-cycles Ru films. A good agreement between the data and the fit was achieved in the range of 3.0–6.5 eV. However, a strong Drude absorption present for the 60-cycle Ru film hindered convergence for the fitting of thinner Ru films in the 0.6–3.0 eV spectral range.

Based on these observations, a fit was performed on the oscillator parameters with resonances below 3 eV, while keeping the rest of the oscillator parameters fixed. The results are shown in Figs. 1(b) and 1(c) and the fit parameters are summarized in Table II. The resulting dielectric constants are presented in Fig. 2 in grey. The model for the fits of 27-cycles of Ru ALD is shown in the upper inset of Fig. 1, and the model for both 12 and 20 cycles of Ru ALD is shown in the lower inset of Fig. 1. The difference between the two models is that for the 27–60 cycle Ru films, the effective medium approach results in a better convergence when the top layer involves a nonabsorbent dielectric function of $n = 1.48$ and $k = 0$, such as a film with a large concentration of precursor impurities.[1] For a lower number of ALD cycles, fewer organic impurities originating from the Ru precursor are accumulated in that layer;[1] consequently, for 12–20 cycles of Ru ALD, the best-fit is achieved when the

TABLE II. Thickness correlation data based on RBS and ellipsometry. For ellipsometry, the data correspond to the model shown as an inset in Fig. 1. All samples were modeled by the identical models for consistency. However, for thick Ru films, similar goodness of fit was achieved when replacing the interface-model by a single layer of Ru/precursor (or equally Ru/SiO_2) phases. This resulted in 13 nm EMA-modeled Ru layer with 87% Ru for 60 c. sample and 10 nm Ru EMA-layer of 90% Ru for 56 c. Ru sample. All data are shown with 15% accuracy.

			Ru Top layer		Ru/SiO_2 interface	
	RBS Ru thickness[23] (nm)	Ellipsometric Ru thickness (based on Eq. (6)) (nm)	Layer thickness (nm)	Ru composition (%)	Layer thickness (nm)	Ru composition (%)
60 cycles	9	11.4	6.4	84	6.4	94
56 cycles	8	9.2	5.3	92	5.3	82
27 cycles	4.1	4.6	4.1	82	4.1	30
20 cycles	2.5	2.9	1.9	95	5.4	20
12 cycles	1.7	1.95	1.5	70	5.0	18

dielectric function of air (n = 1) is incorporated within the effective medium approximation. In all EMA-based fits, however, the interface was made up of SiO_2 and Ru phases. Similar to the thicker films, the effective dielectric function obtained for thinner films (Fig. 2, grey) shows a good agreement with literature values[17] at higher frequencies. Strong deviations are observed in 0.6–2.5 eV spectral range, due to the suppressed charge carrier response in Ru islands as compared to a thick Ru film.

B. Composition and thickness

This section addresses the composition and thickness of the Ru films and interfacial regions. We compare the results obtained from the fits of the ellipsometric data based on the effective medium models with the information provided by the RBS, XPS, and XRD measurements. This allows us to evaluate the Ru fraction *f* for further evaluation of the resistivity using the Landauer theory Eq. (4).

Table II suggests that for the thick (56–60 cycles) Ru films, the thicknesses of the top Ru layer are in the range of 5.3–6.4 nm with a Ru concentration of 84% to 92%. The overall Ru ellipsometric thickness as calculated from Eq. (6) is in close agreement with the Ru thicknesses estimated from RBS measurements. The discrepancies between the RBS and the ellipsometric data arise from the fact that: (1) the evaluation of the interfacial composition becomes less accurate as the thickness of the top Ru layer becomes larger due to the limited penetration depth[22] of the probing radiation through the metallic layer—e.g., the penetration depth for Ru at 3 eV under the normal angle of incidence is around 14 nm—and (2) a lower limit on the Ru thickness is set by the assumption of a bulk Ru density[23] when evaluating the Ru thickness from RBS measurements. Indeed, in accordance with Table II, the RBS Ru thicknesses are consistently lower than those obtained from ellipsometry for all of the examined samples.

The interfacial concentration of Ru in the SiO_2/Ru layer gradually increases from the thinnest films (18% of Ru for 12 c.) to the thickest films (94% of Ru for 60 c.). However, the interface is likely to include additional compounds, such as the residual precursor (as supported by IR data in Ref. 1). Since the refractive index of SiO_2 (in the relevant spectral range) is close to that found for the range of organic materials,[24] it is not possible to distinguish between these two materials.

In the initial stages of Ru deposition (12–27 cycles), the interface layer is well modeled by a 4–5.5 nm thick SiO_2/Ru interface with 18%–30% of Ru. This model emphasizes the roughness of the interface as the initially H-passivated Si surface oxidizes at the same time as the Ru islands form. For a higher number of ALD cycles (56–60 c.), the interface is modeled by an 82%–94% Ru composition. Replacing the interface-model by a single layer of Ru/precursor (or equally Ru/SiO_2) phases results in 13 nm EMA-modeled Ru layer with 87% Ru for the 60 c. sample and 10 nm Ru layer of 90% Ru for the 56 c. Ru sample with a comparable goodness-of-fit measure.[25] This is not the case for thinner films (12–27cycles). In these films, removal of the interfacial layer and fitting on a single Ru film either with Ru/air or Ru/SiO_2 composition result in the deterioration of the goodness of fit by a factor of 3 or higher, depending on the sample. This points to the formation of a rough interface at the initial stages of Ru deposition.

To better address the interfacial composition, the deconvoluted Si2p and Ru3d core-level spectra are shown in Fig. 3 for 12c. and 27 c. Ru films. Fig. 3(a) shows data from the piranha-cleaned Si oxide surfaces, and Fig. 3(a-1) shows the data obtained after 6 min of sputtering of the pure bulk Ru sample, for comparison. The XPS data present clear evidence for the formation of SiO_2 at the interface. The XPS spectra in the 278–288 eV range consist of two contributions: the C1s core-level and the Ru3d core-level. Thus, the sputtered bulk Ru surface can be used as a clean-reference (free of oxygen—as confirmed by the absence of the O1s—and of carbon) to test the deconvolution of the Ru3d core levels of the ALD Ru films. While the Ru3d core-level data obtained from the sputtered bulk Ru sample did not require any additional component to be fitted (Fig. 3(a-1)), an additional peak due to carbon was required to fit the ALD-deposited Ru thin films. The absence of the RuO_2 peaks (expected 0.65 eV higher relatively to the position of the $Ru3d_{5/2}$ peak[26]) in XPS data is in agreement with the XRD spectra (Fig. 4) that are devoid of any RuO_2 phase (in agreement to the XRD data published by Leick *et al.*[2]). The C1s peak position due to the residual carbon was deconvoluted in the 284–285 eV range, to account for CO and CH_x species that constitute the Ru precursor.[1,27]

To summarize this section, XRD, XPS, and ellipsometric data point out on the formation of Ru films that do not contain RuO_2 phases, in accordance with the earlier observations by Leick *et al*. The formation of SiO_2 at the interface, as deduced from the XPS data, is consistent with the observations of the SiO_2 absorption bands in the IR spectra previously reported during the growth of Ru thin films.[1] Not surprisingly, therefore, the best-fit of the ellipsometric data of thinner Ru films (12–27 ALD cycles) was achieved using the EMA model wherein the interface consisted of SiO_2 and 18%–30% of Ru phase. The necessity to model the interface and the topmost layer by EMA models emphasizes the presence of an interfacial layer and of surface roughness within this interface.

C. Sheet resistance

In this section, the parameters of the Ru film structure and composition that were obtained in Secs. III A and III B

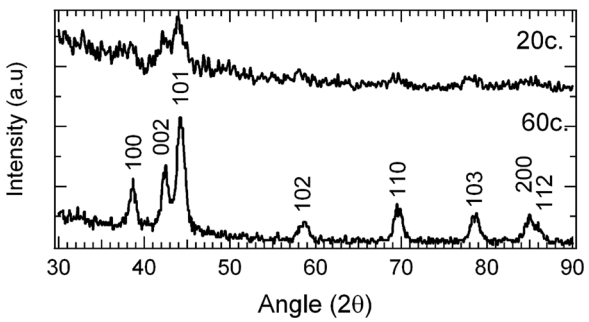

FIG. 4. XRD data obtained from 20 cycle-ALD Ru film and 60-cycle Ru film. Similar peaks are observed in both data sets.

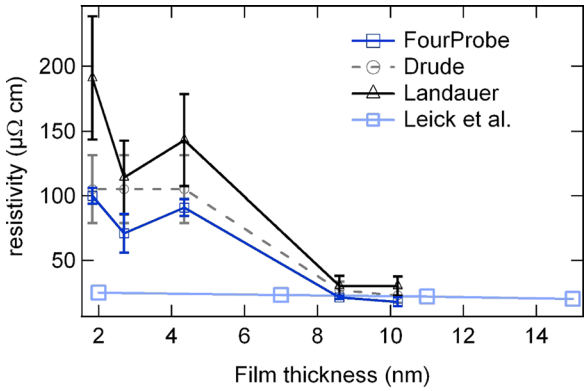

FIG. 5. Resistivity data based on FPP measurements (dark blue); Landauer theory (black), and the data reproduced with permission from N. Leick *et al*., J. Vac. Sci. Technol. A **29**, 021016 (2011). Copyright 2011, American Vacuum Society, showing thermal ALD Ru films deposited on TiN, for comparison (light blue). The broken grey line represents data calculated based on Drude model Eq. (3). The average film thickness (in our experiments) was obtained from RBS and ellipsometric data.

are used for evaluating the Ru resistivity and compared to the 4-probe measurements data.

Substituting the values of w_p and Γ_d from Table I in Eqs. (2) and (3), the Drude-derived resistivity of the Ru islands can be calculated. Using these data along with the fraction f_1 of the Ruthenium phase ($f_{Ru\ top}$, tabulated in Table II) as an input into the Landauer model Eq. (4), the ellipsometry-derived DC-resistivity, ρ_{opt} is then obtained. The conductivity σ_1 of the second phase (essentially an insulator in our case) is very small in comparison to the metallic phase, and the results are insensitive to whether the resistivity values of air or of a material similar to SiO_2 of ρ varying between 10^{14} Ωm and 10^{16} Ω m are used as an input.

The resistivity values derived from the Landauer theory are summarized in Fig. 5 (in black) along with the data obtained from the electrical FPP measurements (dark blue). The Drude values for the resistivity of the Ru islands, derived from Eqs. (2) and (3), are shown for comparison by a broken grey line.

The resistivity values obtained from the Landauer model are consistently higher than the electrically measured sheet resistance values. The best agreement is achieved for the thicker films (56–60 ALD cycles), where the composition of Ru films is better defined and the error bar is smaller. For the thinnest film (12 c. ALD), the Landauer values do not match the electrically measured resistivity although they are still of the same order-of-magnitude as what is obtained from the 4-probe measurements. There are several possibilities for this observation. First, the inputs into the Landauer equations strongly depend on the ellipsometric evaluation of the Ru composition and of the dielectric function. As we have already mentioned in Sec. III B, the surface and the interface structure of the Ru films are complex at the initial stages of Ru deposition. Although the proposed ellipsometric models describe well the ellipsometric signal, they are limited by the following *assumptions*: (1) the existence of *abrupt* interfaces between the layers; and (2) a constant composition of the EMA-related phases throughout the whole thickness of the film. In fact, the thinner the films, the more poorly these surfaces and interfaces are defined. The discrepancy between the Landauer values and the FPP measurements for the 12-cycles Ru films indicates that the ellipsometric models probably underestimate the Ru concentration in the top-most layer. This discrepancy can also be related to the particular differences between the two measurement methods: while the FPP measures the overall film resistivity in a parallel circuit, where the current flows in a favorable conduction path, the ellipsometric models provide average values over the given layers. Thus, it is not surprising that the FPP measurement yields smaller values. This effect perhaps enlarged by a partial percolation of the Ru in the films.[28]

A thickness-dependent resistivity was also observed for Ta deposited on TaN by Rudra *et al*.[7] who attributed the changes in resistivity to the crystallographic variations of Ta, with the α-phase of Ta becoming more prominent with increasing thickness. This is not the case for Ru films since the XRD data obtained from both the 20-cycles and the 60-cycles Ru films Ru films are identical (see Fig. 4).

On the other hand, Leick *et al*.[2] observed a much lower thickness-dependent behavior than in our films for Ru films deposited on TiN substrates using a similar ALD process, although there is a good agreement between our data and the data presented by Leick *et al*.[2] for *thick* Ru films. As the films become thinner, the resistivity of Ru deposited on Si increases strongly, while the resistivity values of Ru deposited on TiN stay relatively low. These differences cannot be attributed to the crystallographic structure of the deposited Ru because the XRD data of Ru deposited on Si in our case are identical to that published by Leick *et al*.[2] The most likely cause for the differences of the resistivity dependence as a function of Ru thickness is the difference in the growth mechanism on Si and TiN. The most plausible explanation for the observed thickness-dependent resistivity is the island-growth of Ru on originally H-passivated Si surfaces, where isolated islands are formed at the initial stages of Ru deposition and then slowly coalesce as the number of the ALD cycles increases. This hypothesis is supported by a recent publication by Yim *et al*.,[11] whose results indicate that the nucleation of Ru islands on nitride (SiN_x) surfaces is significantly enhanced in comparison to nucleation of Ru islands on SiO_2 surfaces.

IV. CONCLUSIONS

In conclusion, we have shown that the resistivity of thin metallic films evaluated from the ellipsometric optical response using the Landauer theory can be correlated to the sheet resistance obtained by the direct electrical 4-point probe measurements when care is taken to determine the precise effective-medium composition of the top layer. The island-growth mechanism of Ru on originally H-passivated Si results, however, in a complex surface and interface structure at the initial stages of atomic-layer deposition. Consistent with our earlier published IR spectra,[1] the ellipsometric data suggest the formation of a rough SiO_2/Ru interface during the initial Ru-ALD cycles. These initial stages of Ru growth on Si are characterized by a conductivity lower than

that observed for Ru grown on TiN substrates for similar film thicknesses. This observation is consistent with the earlier studies[11] indicating that the nucleation of Ru islands on nitride surfaces is significantly enhanced in comparison to nucleation of Ru islands on SiO_2 surfaces. With increasing Ru thickness, the measured conductivity approaches Ru resistivity values similar to those obtained by other groups on TiN[2].

ACKNOWLEDGMENTS

This work was supported by the National Science Foundation (Grant No. CHE-0911197) and partially by the Texas Higher Education Coordinating Board NHARP Program.

[1]S. K. Park, R. Kanjolia, J. Anthis, R. Odedra, N. Boag, L. Wielunski, and Y. J. Chabal, Chem. Mater. **22**, 4867 (2010).
[2]N. Leick, R. O. F. Verkuijlen, L. Lamagna, E. Langereis, S. Rushworth, F. Roozeboom, M. C. M. van de Sanden, and W. M. M. Kessels, J. Vac. Sci. Technol. A **29**, 021016 (2011).
[3]K. Gregorczyk, L. Henn-Lecordier, J. Gatineau, C. Dussarrat, and G. Rubloff, Chem. Mater. **23**, 2650 (2011).
[4]M. Schuisky, Appl. Phys. Lett. **81**, 180 (2002).
[5]E. Langereis, S. B. S. Heil, H. C. M. Knoops, W. Keuning, M. C. M. van de Sanden, and W. M. M. Kessels, J. Phys. D: Appl. Phys. **42**, 073001 (2009).
[6]W. S. Choi, S. S. A. Seo, K. W. Kim, T. W. Noh, M. Y. Kim, and S. Shin, Phys. Rev. B **74**, 205117 (2006).
[7]S. Rudra *et al*., Phys. Status Solidi A **205**, 922 (2008).
[8]X. L. Wang, T. Nanba, M. Ikezawa, Y. Isikawa, K. Mori, K. Kobayashi, K. Kasai, K. Sato, and T. Fukase, Jpn. J. Appl. Phys., Part 2 **26**, L1391 (1987).
[9]P. Yu and M. Cardona, *Fundamentals of Semiconductors* (Springer, Heidelberg, 2010).
[10]R. Landauer, J. Appl. Phys. **23**, 779 (1952).
[11]S.-S. Yim, D.-J. Lee, K.-S. Kim, S.-H. Kim, T.-S. Yoon, and K.-B. Kim, J. Appl. Phys. **103**, 113509 (2008).
[12]*Handbook of X-ray Photoelectron Spectroscopy*, edited by C. D. Wagner, W. M. Riggs, L. E. Davis, J. F. Moulder, and G. E. Muilenberg (Perkin-Elmer, Corp., Eden Prairie, MN, 1979).
[13]S. Lizzit *et al*., Phys. Rev. B **63**, 205419 (2001).
[14]S. Huefner and G. K. Wertheim, Phys. Rev. B **11**, 678 (1975).
[15]D. Stroud, Superlattices Microstruct. **23**, 567 (1998).
[16]G. A. Niklasson, C. G. Granqvist, and O. Hunderi, Appl. Opt. **20**, 26 (1981).
[17]E. D. Palik, *Handbook of Optical Constants of Solids* (Academic, San Diego, 1998).
[18]G. E. Jellison, Jr., Opt. Mater. **1**, 41 (1992).
[19]P. Lautenschlager, M. Garriga, L. Vina, and M. Cardona, Phys. Rev. B **36**, 4821 (1987).
[20]G. E. Jellison and F. A. Modine, J. Appl. Phys. **76**, 3758 (1994).
[21]M. Kildemo, R. Ossikovski, and M. Stchakovsky, Thin Solid Films **313–314**, 108 (1998).
[22]The penetration depth is defined here as the power decay to $1/e^2$ of the initial value at a normal angle of incidence. The penetration depth is then $\delta_\varepsilon = [(\omega / c)\mathrm{Im}(n^*(\omega))]^{-1}$ where ω is the angular frequency of the incident radiation, c is the speed of light, and $\mathrm{Im}(n^*(\omega))$ is the imaginary part of the complex refractive index.
[23]RBS thickness was calculated based on 12.45 g cm.
[24]D. E. Gray, S. C. Case-Green, T. S. Fell, P. J. Dobson, and E. M. Southern, Langmuir **13**, 2833 (1997).
[25]G. E. Jellison, Appl. Opt. **30**, 3354 (1991).
[26]R. Blume, M. Haevecker, S. Zafeiratos, D. Teschner, A. Knop-Gericke, R. Schloegl, P. Dudin, A. Barinov, and M. Kiskinova, Catal. Today **124**, 71 (2007).
[27]Since the deconvolution is hindered by the overlap between the Ru3d and the C1s XPS peaks, the C1s peak position was allowed to vary in the 284–285 eV range to account for chemical shift due to the precursor-related aliphatic and the CO-type of the residual carbon. At the same time, the components of the Ru3d were kept strictly with the $Ru3d_{5/2}$ component positioned at 280 eV, keeping spin-orbit splitting of 4.22 eV with ratio of 2:3. The freedom provided for variation of the C1s component results in a shift of the carbon-related component in Figs. 3(b-1) and 3(c-1). This shift may be related to the different amounts of CH_x and CO species (related to the precursor) at different stages of the ALD deposition.
[28]B. Gompf, J. Beister, T. Brandt, J. Pflaum, and M. Dressel, Opt. Lett. **32**, 1578 (2007).